# Characterization of *FLOWERING LOCUS T* related genes and their putative gene regulatory network in semi-winter *Brassica napus* cultivar Zhongshaung11

Juanjuan Wang[1], Hao-Ran Zhou[1], Jing Wang[2], Franziska Turck[1]#

[1]Max Planck Institute for Plant Breeding Research, Carl von Linné Weg 10, 50829 Köln

[2]MOA Key Laboratory of Crop Ecophysiology and Farming System in the Middle Reaches of the Yangtze River, College of Plant Science and Technology, Huazhong Agricultural University, Wuhan, PR China. wangjing@mail.hzau.edu.cn

#author for correspondence turck@mpipz.mpg.de

Franziska Turck (ORCID 0000-0002-4982-5949)

Juanjuan Wang (ORCID 0000-0002-1142-6643)

Hao-Ran Zhou (ORCID 000-0001-5945-2448)

Jing Wang (ORCID 0000-0002-7103-8511)

## Summary

Flowering time is a crucial phenological trait with a direct influence on biomass and seed yield of crop plants. In many plant species, *FLOWERING LOCUS T* (*FT*)-like genes promote transition to flowering by integrating environmental signals, in particular photoperiod, and internal cues.

- *Brassica napus* contains eight *FT*-like genes, of which four are orthologs of *FT*, one functional and two pseudogenes belong to an Brassicacae linage II-specific and one gene to a Brassica C-genome-specific orthogroup.
- All six extant *FT*-like genes induce early flowering in *ft* mutant background if expressed at the shoot apex, but only three orthologs are fully functional as mobile florigens.
- BnaFT.C6 was not fully functional al mobile florigen. A change of the last amino-acid from threonine to cysteine contributes to the reduced function and is private to a subset of semi-winter accessions

- Both distal enhancers of *FT* were found at all four syntenic genes in *B. napus*; however, homeologs *BnaFT.A7* and *BnaFT.C6* showed rearrangements of DNA-motifs binding NF-Y/CO and NF-Y transcription activator complexes between the proximal promoter and the downstream enhancer Block E.
- Homeologs with rearranged motifs could not be trans-activated by *B. napus* CO in transient reporter assays
- All *FT* orthologs were dependent on long day photoperiod and vernalization. Homeologs with rearranged and canonical motif arrangement showed higher transcript levels in vegetative and paraclade leaves, respectively
- Diurnal transcriptome data of leaves from *B. napus* plants grown in SD and LD photoperiod indicate that a large group of NF-Y encoding genes show a peak of expression in the critical phase between ZT12 and ZT16, exclusively in LD.

In sum, *B. napus* photoperiod dependent regulation of *FT*-like genes is a case study for the consequence of gene duplications, indicating gene retraction through loss-of-function, homeolog retention partially explained by differences transcriptional regulation and possibly variation between cultivated varieties due to changes in protein function.

Key words: FLOWERING LOCUS T, *Brassica napus*, flowering time, transcriptional regulation, CONSTANS, NF-Y

# Introduction

Flowering is an important growth stage in plants with direct impact on biomass, survival and seed production and hence crucial for crop yield. Flowering is promoted by environmental and developmental signals in angiosperms and based on observations made in the model plant *Arabidopsis thaliana,* the underlying flowering promoting pathways have been categorised as the vernalization, photoperiod, autonomous, gibberellin (GA) and age pathways (Andrés & Coupland, 2012; Teotia & Tang, 2015). A major integrator of flowering cues in *A. thaliana* is *FLOWERING LOCUS T* (*FT*), which plays a pivotal role in the photoperiod pathway but also senses cues from other pathways (Bratzel & Turck, 2015; Takagi *et al.*, 2023). FT acts as a mobile florigen, as it is transcribed in the phloem companion cells of leaves in response to a long day (LD) photoperiod. This subsequently allows FT protein to move as a protein through sieve elements to the shoot apical meristem (SAM), where it associates with the transcription factor FLOWERING LOCUS D (FD). The FT/FD complex directly promotes the expression of genes that switch the developmental program of the SAM from vegetative to reproductive growth (Abe *et al.*, 2005; Wigge *et al.*, 2005; Jaeger & Wigge, 2007).

*FT*-like genes were shown to promote flowering in many plant species; furthermore, as mobile signals they can also impact inflorescence commitment and architecture, shoot branching, storage organ formation and seed dormancy, underscoring their importance for plant fitness (Jin *et al.*, 2021a). Many plant species show *FT*-like gene expansion, such as the *FT* paralog *TWIN SISTER OF FT* (*TSF*) in *A. thaliana*, which has diversified in expression but not protein function (Yamaguchi *et al.*, 2005). Functional diversification of paralogs has also been reported; for example, *BvFT2* and *BvFT1* in *Beta vulgaris* (sugar beet) respectively activate and repress flowering, which is crucial to integrate vernalization to flowering regulation in this species (Pin *et al.*, 2010).

Research on the transcriptional regulatory mechanisms of *FT* uncovered a network of activating and repressing transcription factors, epigenetic regulators and cis-acting regulatory elements (Bratzel & Turck, 2015; Takagi *et al.*, 2023). *FT* activation in LD requires the combined input of the proximal promoter and two distal transcriptional enhancers, located at 5.7-kb and 1.6-kb distance up- and down-stream of the structural gene, respectively (Adrian *et al.*, 2010; Tiwari *et al.*, 2010; Cao *et al.*, 2014; Liu *et al.*, 2014; Zicola *et al.*, 2019). *FT* regulatory regions recruit related protein complexes: the canonical ternary eukaryotic CCAAT box binding factors (CBF), also known as NF-Y complexes and related plant-specific NF-Y/CO complexes. NF-Y complexes bind CCAAT motifs and are composed of one of each NF-YB, NF-YC and NF-YA subunits.

81 In NF-Y/CO complexes, the NF-YA component is replaced with the plant-specific
82 CONSTANS, CONSTANS-like, TOC1 (CCT) domain protein CONSTANS (CO). CCT
83 domains exhibit structural similarity to NF-YA, yet demonstrate direct, high-affinity binding to
84 CCACA in lieu of CCAAT motifs (Wenkel *et al.*, 2006; Gnesutta *et al.*, 2017; Lv *et al.*, 2021).

85 Photoperiod regulation in plants involves transcriptional and post-transcriptional control of CO.
86 Transcriptional control includes the degradation of CO's repressors, such as CYCLIC DOF
87 FACTOR 1-LIKE (CDFs), by a blue light receptor complex that contains FKF1 and
88 GIGANTEA (GI) (Imaizumi *et al.*, 2005; Sawa *et al.*, 2007; Fornara *et al.*, 2009). CO transcription is
89 repressed in the morning and activated in the late afternoon. CO protein decreases in the night
90 due to CONSTITUTIVE PHOTOMORPHOGENESIS 1 (COP1) and SUPPRESSOR OF
91 PHYA-105 (SPA) 1-4 proteins (Laubinger *et al.*, 2006; Jang *et al.*, 2008), while photoreceptors
92 regulate CO stability throughout the day (Yanovsky & Kay, 2002; Valverde *et al.*, 2004; Posé *et al.*,
93 2013). This regulation allows CO protein to accumulate at dusk under LD but not short day (SD)
94 photoperiod. Additionally, other transcription factors like PHYTOCHROME INTERACTING
95 FACTORs (PIFs) and CRYPTOCHROME 2-INTERACTING bHLH (CIB) proteins modulate
96 *FT* expression in response to light and temperature (Kumar *et al.*, 2012; Liu *et al.*, 2013, 2018;
97 Fernández *et al.*, 2016; Galvão *et al.*, 2019).

98 A strong motivation for in-depth studies in genetic model organisms is the potential for
99 translational application to crops. While key pathway integrators are mostly conserved, how
100 these are embedded in gene regulatory networks can diverge even between closely related
101 species. The Brassica genus includes important crops, which diverged from *A. thaliana* 27
102 million years ago. The genus underwent a genome triplication and differentiated three lineages,
103 designated as type A, B and C genomes (Kagale *et al.*, 2014). Detailed comparison of synteny
104 between and within these genomes revealed the presence of a least fragmented (LF) genome
105 and two genomes that were mildly (MF1) or mostly fragmented (MF2) with rearrangements
106 often resulting in gene loss (Parkin *et al.*, 2005; Cheng *et al.*, 2013). Hybrids between Brassica
107 lineages were strongly favoured by early farmers in their selection of crops. The most important,
108 *Brassica napus* (AACC, 2n=38) is mostly grown as oilseed rape (canola) and originated around
109 7,500 years ago through hybridization between the diploid progenitors *Brassica rapa* (AA,
110 2n=20) and *Brassica oleracea* (CC, 2n=18), probably in the Mediterranean region (Chalhoub,
111 2014; Wu *et al.*, 2019; Lu *et al.*, 2019). The global *B. napus* gene pool has undergone several post-
112 domestication ecogeographic radiations, which provided the origin of three cultivars according
113 to their vernalization requirements (Zou *et al.*, 2019). Winter rapeseed is mainly found in Europe

114 and requires a prolonged period of low temperatures to transit from vegetative to reproductive
115 growth; semi-winter rapeseed, mainly produced in China, can initiate flowering after a shorter
116 vernalization period; and spring rapeseed, which presents a wide distribution in Northern
117 Europe, Canada, and Australia, can flower and reproduce without vernalization.

118 Previous studies have shown that gene groups involved in flowering regulation in *A. thaliana*
119 show both expansion and retraction in *B. napus*, indicating that purifying and diversifying
120 selection takes place. In the case of *FT*, six or seven homologs were identified, depending on
121 study and genetic background (Schiessl *et al.*, 2014; Schiessl, 2020). Notably, silencing of a *FT*
122 syntenic *B. napus* gene on chromosome C02 (*BnaFT.C2*) coincided with two TE insertions
123 between the proximal promoter and consequent high levels of cytosine methylation in TE
124 sequences within proximal promoter region (Wang *et al.*, 2012a). Three *BnaFT* paralogues,
125 designated as *BnaA2.FT*, *BnaC6.FT.a* and *BnaC6.FT.b* were associated with two major QTL
126 clusters for flowering time, in a mapping population from the cross of the winter-type cultivar
127 Tapidor and the semi-winter cultivar NY7 (Wang *et al.*, 2009). Analysis of selective sweeps
128 between spring, semi-winter and winter ecotypes, and GWAS for flowering time confirmed
129 that *BnaFT.A2* (*BnaA02g12130D*) is significantly associated with flowering-time variation (Wu
130 *et al.*, 2019). In addition, EMS-induced mutant alleles of *BnaC6.FT.b* exhibited delayed
131 flowering compared to the control group, while mutants of *BnaC6.FT.a* exhibited flowering
132 patterns akin to the non-mutated parent in winter-type inbred line Express 617 (Guo *et al.*, 2014).
133 Furthermore, loss-of-function mutants in Westar and RNAi lines in Tapidor of *BnaFT*.A2 have
134 smaller leaves, a lower net photosynthetic rate, as well as a substantial delay in flowering time
135 compared to their parents (Jin *et al.*, 2022).

136 Here we present a comparative analysis of six *FT*-like genes encoded by the semi-winter *B.*
137 *napus* cultivar Zhongshaung11 (ZS11).

# 138 Materials and Methods

139 **Plant material and growth conditions**

140 *A. thaliana* accession Columbia (Col-0) and the *ft-10* T-DNA insertion mutant (GABI-Kat line
141 290E08) were cultivated in a temperature-controlled greenhouse in LD photoperiod (20-24°C,
142 16h light/8h dark) on soil. *B. napus* cultivar ZS11 plants were grown in the greenhouse (20-
143 24°C) for the collection of tissues from different growth stages and in growth chambers (CLF
144 Plant Climatics, AR-95L3X, 60% light intensity (12570 LUX), 75% relative humidity. 22°C)
145 under LD (16 h light /8 h dark) or SD (8 h light /16 h dark) for the collection of leaf material

146 for diurnal transcriptomes. For vernalization, plants were moved to vernalization rooms (4°C,
147 SD).

148 **Identification of *BnaFT* and *NF-Y* homologs in *B. napus***

149 Synteny analysis was performed using the MCscan algorithm (Wang *et al.*, 2012b) as
150 implemented in the JCVI toolkit (Tang *et al.*, 2024). Genome sequences and genome annotations
151 for *B. napus* (ZS11.v0) and *Brassica oleracea* var capitata (JZS.v2) (BnPIR;
152 http://cbi.hzau.edu.cn/bnapus) (Song *et al.*, 2020), *Brassica rapa* Z1_v2
153 (https://www.genoscope.cns.fr/externe/plants/data/), *Schrenkiella parvula* v2.2 (Phytozome13;
154 https://phytozome-next.jgi.doe.gov/) and *A. thaliana* Col-0 Araport11 (TAIR;
155 https://www.arabidopsis.org/) were downloaded from the indicated sources. Amino acid
156 sequences of annotated proteins were generated using the scripts of the JCVI toolkit and blasted
157 all against all using the LAST algorithm (Kiełbasa *et al.*, 2011). To identify syntenic genes, 6
158 iterations of comparing all genomes against the *A. thaliana* and *S. parvula* genomes by MCscan
159 were performed.

160 Homologs of FT (AT1G65480) (Supplemental Table 1) and NF-Y proteins (Supplemental
161 Table 2) in *B. napus* var ZS11 were identified using screen criteria of E-value ≤ 1.0E-20,
162 coverage ≥ 95%, identity ≥ 80%. *FT*-like pseudogenes were identified by relaxing the coverage
163 criteria. To include them in the alignment, frameshift mutations and stop codons were corrected
164 according to the output of the Scipio webtool (Hatje *et al.*, 2011). To construct a phylogenetic tree
165 of FT-like proteins, full length protein sequences of FT, TSF, TFL1, BFT and MFT from *A.*
166 *thaliana* were obtained from TAIR database (https://www.*arabidopsis*.org/). Protein
167 alignments were performed with ClustalW and a 60% majority-rule consensus tree was
168 constructed from a bootstrapped (n=1000) neighbor joining (NJ) using MEGA11 (Tamura *et al.*,
169 2021). NF-Y proteins were aligned and visually curated with ClustalW. An maximum-
170 likelihood phylogenetic tree was generated that included *A.thaliana* and *B.napus* homologs of
171 all three NF-Y families for overview.

172 **mVISTA analysis**

173 Genomic sequences including upstream and downstream sequences up to the next flanking
174 genes were submitted to the mVISTA webtool for alignment
175 (https://genome.lbl.gov/vista/mvista/submit.shtml).

176 **Annotation of cis-regulatory motifs at conserved regulatory regions**

177 Sequences identified as aligning to conserved Blocks C, A and E were extracted and re-aligned
178 using ClustalW in MEGA11 (Tamura *et al.*, 2021). Motifs were annotated and plotted using
179 custom scripts in R.

180 **Plasmids construction for complementation and transient expression**

181 The vector *(C+A)-FTpromoter(FTp)-FTcDNA-pGreen* and transgenic *(C+A)-FTp-FTcDNA-*
182 *pGreen/ft-10* plants were described previously (Liu *et al.*, 2014). Full length coding sequences of
183 *BnaFT.A2*, *BnaFT.C2*, *BnaFT.A7*, *BnaFT.C6*, *BnaNFT.A7*, and *BnaCFT.C4* were amplified
184 from ZS11 cDNA using primer pairs as indicated in Supplemental Table 2. PCR products were
185 introduced into *(C+A)-FTp-FTcDNA-pGreen* (Liu *et al.*, 2014) via *Hind*III and *Sac*I restriction
186 enzyme sites to replace the original *FT* CDS on the backbone using NEBuilder® HiFi DNA
187 Assembly Master Mix according manufacturer's instructions (NEB, Frankfurt, Germany).
188 For expression of *FT*-like genes at the shoot apex, the vector *FDp-FD-3xVENUS-pER8* was
189 used as backbone. Full-length coding sequences were amplified with two rounds of PCR to
190 add an N-terminal HA-epitope to the full-length sequence using primers as indicated in
191 Supplemental Table 3. Similarly, the mutant versions of *BnaFT.A7* and *BnaFT.C6*, namely
192 *BnaFT.A7*m and *BnaFT.C6*m, were amplified using vectors *(C+A)-FTp-BnaFT.A7-pGreen* and
193 *(C+A)-FTp-BnaFT.C6-pGreen* as the templates. The final PCR products were inserted into
194 vector backbone FDprom-FD3V-pER8 using *Xho*I restriction enzyme sites using NEBuilder®
195 HiFi DNA Assembly Master Mix.
196 For luciferase (LUC) reporter vectors, a cassette containing the *CaMV 35S* promoter (*35Sp*)
197 and *Renilla Luciferase (RLUC)* was inserted into *BlockA-FTp-LUC68-pGreen* (Adrian *et al.*,
198 2010) via *Eco*RI restriction enzyme sites using Gibson assembly. Promoters of *BnaFT.A2*,
199 *BnaFT.A7*, *BnaFT.C6* were amplified from ZS11 gDNA using primer pairs listed in
200 Supplementary Table 3 and introduced via *Sca*I and *Nco*I restriction enzyme sites to replace the
201 *Block A FT* promoter using Gibson assembly. For effector vectors, the cassettes *35Sp-*
202 *BnaCO.A10* and *35Sp-BnaCO.C9* were introduced into the vector *BlockA-FTp-LUC68-pGreen*
203 via restriction enzyme sites *Sca*I and *Sac*I using Gibson assembly, to replace Block *FTp-*
204 *LUC68*. For transient LUC reporter assays, the vectors *35Sp-LUC68-pGreen* and *35Sp-H2B-*
205 *pGreen* were used as positive and negative controls, respectively.

206 **Plant transformation**

207 Plasmids were introduced into *Agrobacterium tumefaciens* strain GV3101(pSoup) to transform
208 *ft-10* by floral dipping (Clough & Bent, 1998). Transformants were selected on soil by applying
209 Basta (glufosinate) spray (0.1%) twice for the vectors using *(C+A)-FTp-FTcDNA-pGreen* and

210 on plates supplemented with hygromycin (50 mg/L) for the vectors using *FDp-FD3V-pER8* as
211 the backbone.

212 **Tobacco infiltration and luciferase assay**

213 The cell suspension of *A. tumefaciens* GV3101(pSoup) strain carrying the plasmids of interest
214 was mixed according to the experimental design and then infiltrated into the underside of the
215 *N. benthamiana* leaves as described (Sparkes *et al.*, 2006) with the following adjustments: 10 mM
216 MES and 40 μM acetosyringone were added to the *A. tumefaciens* culture, which was then
217 incubated overnight at 28°C. The culture was then centrifuged at 4,000 *g* for 15 min and the
218 supernatant was replaced with the infiltration medium. *A. tumefaciens* culture was then placed
219 at room temperature for at least 3 h before being used for infiltration. At 48 h after infiltration,
220 infiltrated *N. benthamiana* leaves were excised and sprayed with triple-diluted Luciferase Assay
221 Reagent (Promega E1500). Fluorescence signal images were taken at least 10 min later with
222 the ChemiDoc Imaging System (Bio-Rad). If signals were observed, the infiltrated leaf spots
223 were sampled with a punch and transferred into 1.5-mL Eppendorf tubes containing magnetic
224 beads (the diameter of 0.32 cm). The samples were snap-frozen in liquid nitrogen and were
225 stored at -80°C for subsequent signal quantification. Frozen samples were ground with the
226 TissueLyser II (QIAGEN) for 1 min at 30 Hz. Then, 150 μL of 1× lysis reagent (Promega
227 E1500) was added to the sample, which was mixed and then centrifuged at full speed with a
228 bench-top 5427 R centrifuge (Eppendorf) for 1 min. A 60 μL portion of the supernatant was
229 transferred to a 96-well plate. An equivalent volume (60 μL) of Dual-Glo® Luciferase Reagent
230 (Promega E2920) was added to each well and mixed with the sample. After at least 10 min, the
231 firefly luminescence was measured using a multimode reader TriStar² LB 942 (BERTHOLD).
232 The same volume of 60 μL oDual-Glo® Stop & Glo® Reagent (Promega E2920) was added to
233 each well and mixed with the sample. At least 10 min later, the RLUC luminescence was
234 quantified using the same luminescence reader.

235 **RNA extraction, reverse transcription and quantitative reverse transcribed-PCR (qRT-**
236 **PCR)**

237 For the analysis of tissue-specific expression, *B. napus* cultivar ZS11 were cultivated for 4
238 weeks at 22°C in the greenhouse under LD condition, vernalization for 4 weeks at 4°C in SD,
239 and transferred back to the LD greenhouse. Throughout the developmental progression,
240 sequential samplings of three biological replicates occurred at Zeitgeber time 12 (ZT12). Root
241 and leaf 6 were sampled prior to vernalization, leaf 8, paraclade leaf, floral bud, flower and

242 siliques were sampled after vernalization. Material from leaf 8 was also sampled from non-
243 vernalized plants.
244 For diurnal expression analysis, ZS11 was cultivated for four weeks in separate LD or SD
245 growth chambers, followed by an intervening vernalization period of 4 weeks, after which
246 plants were transferred back to the LD or SD chambers, respectively. Leaf 6 was sampled just
247 before plants were transferred to the vernalization and leaf 8 was harvested one week after
248 transfer to LD or SD chambers at 22°C. Biological triplicates were sampled every 4 hours for
249 24 hours.
250 Total RNA was extracted using the RNeasy Mini Kit (Qiagen, Cat. no. 74104) following
251 manufacturer's instructions. For each sample, 4 µg of total RNA was treated with DNA-free™
252 Kit (Invitrogen, REF AM1906), and cDNA synthesis was performed with Superscript™ IV
253 reverse transcriptase kit (Invitrogen, REF18090050) following manufacturer's instructions.
254 qRT-PCR was conducted in three technical replicates for each biological replicate using the
255 Bio-Rad CFX384™ system (Bio-Rad), technical replicates are shown as median value.
256 The expression levels of *BnaFT.A2*, *BnaFT.C2*, *BnaFT.A7*, *BnaFT.C6*, *BnaNTF.A7*,
257 *BnaCTF.C4*, *BnaCO.A10*, *BnaCO.C9* and *BnaENTH* were tested with gene-specific primer
258 pairs that are listed in Supplemental table 3. Standard curves of each pair of primers were
259 obtained through PCR using gradient-diluted ZS11 genome DNA as the template and Ct values
260 were adjusted using amplification efficiencies prior to using the -ddCt method. The *BnaENTH*
261 gene was used to correct for differences in cDNA concentration, a dilution of genomic DNA
262 was used as common scale for all genes.

263 **Generation and analysis of RNAseq data**

264 Total RNA from three biological replicates of leaf 8 from 24 h time-courses of vernalized *B.*
265 *napus* var ZS11 plants grown in LD and SD were sent to BGI (Hongkong, China) for library
266 preparation and sequencing using the DNBSEQ platform. Reads were aligned to the reference
267 transcriptome using STAR version 2.7.10b (Dobin *et al.*, 2013) and gene expression was
268 quantified as transcript per million (TPM) using RSEM version 1.3.3 (Li & Dewey, 2011).
269 Diurnally expressed genes were identified using Bioconductor R libraries DESeq2 (Dobin *et al.*,
270 2013) and RAIN (Thaben & Westermark, 2014).

# 271 Results

272 **The *B. napus* genome carries four functional *FT* orthologous and two *FT* paralogous genes**

273 A protein similarity search against a high-quality assembly of *B. napus* semi-winter cultivar
274 ZS11 (Song *et al.*, 2020) detected eight FT homologs with identity scores above 81%, of which
275 two were annotated as homologs of TSF but covered the query sequence only partially
276 (Supplemental Table 1). A query of the genomic sequence with the Scipio webtool (Hatje *et al.*,
277 2011) confirmed the presence of six complete *FT*-like genes while proteins showing an
278 incomplete overlap are likely pseudo-genes due to presence of frame shifts and/or non-
279 canonical introns in the predicted coding sequence (Supplemental Table 3, Supplemental Figure
280 1).

281 We compared the linearity of lastal hits between *A. thaliana, S. paruvla*, and *B. napus* genomes
282 using the MCscan toolkit (Tang *et al.*, 2008). *S. parvula* is a diploid representative of the
283 Brassicacea lineage II, which includes the genus Brassica. The analysis confirmed that four *FT*
284 syntenic genes are located on chromosomes A02, C02, A07, and C06 (Wang *et al.*, 2009) (Figure
285 1A, Supplemental Data 1). A *TSF* ortholog was present in *S. parvula* but missing at the
286 corresponding syntenic blocks in *B. napus*, indicating gene loss in the genus Brassica rather
287 than a lineage I specific duplication (Figure 1B). On the other hand, *S. paruvla* and *B. napus*
288 featured an *FT*-like gene at a novel syntenic position on chromosome A07, for which no
289 correspondence could be found in *A. thaliana* (Figure 1C). This gene is a homeolog of both *FT*-
290 like pseudogenes. We propose the name *NEW SISTERS OF FT AND TSF* (*NFT*) to distinguish
291 them from *FT* or *TSF* orthologous genes. *BnaFT.A7*/*BnaNFT.A7* and *BnaFT.C6*/Pseudo-
292 *BnaNFT.C6* are located near a region showing a large inverted duplication in Chromosomes
293 A07/C06 (Parkin *et al.*, 2005); however juxtaposition with the *FT* and *NFT* syntenic segments
294 showed that the *FT* gene is situated at the margin of the original syntenic fragment, narrowly
295 avoiding the duplication (Supplemental Figure 2). A sixth functional *FT*-like gene was located
296 on chromosome C04 at a position unique to *B. napus* and the C-genome parent *B. oleracea*, but
297 absent from *B. rapa*, *S. parvula* and *A. thaliana* (Figure 1D). We propose the name *C-GENOME*
298 *SISTER OF FT AND TSF* (*CFT*) for this gene.

299 A bootstrapped neighbour-joining phylogenetic tree was constructed from the alignment of six
300 functional FT-like proteins, two frame-corrected pseudogenes and FT homologs from *B. rapa*,
301 *B. oleracea*, *S. parvula, A. lyrata* and *A.thaliana*. TERMINAL FLOWER 1 (TFL1), BROTHER
302 OF FT AND TFL1 (BFT) and MOTHER OF FT AND TFL1 (MFT) were added as outgroups
303 (Figure 1E). In this tree, TSF/*Al*TSF clustered together with TSF from *S. parvula* and NFT/CFT
304 proteins indicating a more recent duplication history for non-*FT* orthologs (Figure 1A).

305 **Six extant *B. napus FT* homologs show divergence in their potential to act as mobile**
306 **florigen**
307 To elucidate the potential of FT-like proteins from *B. napus* to act as mobile florigen, the
308 corresponding cDNAs were stably transformed into the *A. thaliana ft-10* mutant under the
309 control of a modified *FT* promoter (*(C+A)-FTp*) that was previously shown to express
310 transgenes in phloem companion cells similar to endogenous *FT* in LD photoperiod (Figure
311 2A) (Liu *et al.*, 2014). *B. napus* genes formed two distinct complementation groups (Figure 2B).
312 *BnaFT.A2*, *BnaFT.A7* and *BnaFT.C2* complemented *ft-10* with delay of 5 to 10 leaves
313 compared to the *FT* control line. Conversely, *BnaNFT/BnaCFT* and *BnaFT.C6* transgenic lines
314 flowered almost as late as *ft-10*. When *B. napus FT*-like genes were expressed directly in the
315 SAM under the control of the *FD* promoter (*FDp*) (Figure 2A) (Abe *et al.*, 2005), independent T1
316 lines expressing *FT* or *B. napus FT* homologs flowered earlier than wild type controls, although
317 a mild but statistically significant delay in flowering was observed within the transgenic lines
318 for *FDp-BnaNFT.A7* and *FDp-BnaCFT.C4* compared to other lines (Figure 2C).

319 The florigenic BnaFT.A7 and the non-florigenic BnaFT.C6 of cultivar ZS11 differ at 5 amino-
320 acid residues, of which none correspond to five FT residues (D17, V18, V70, S76, and R83)
321 previously identified as important for intercellular trafficking (Yoo *et al.*, 2013; Endo *et al.*,
322 2018) (Supplemental Figure 3). The carboxy-terminus is important for FT function, which is
323 abolished by the deletion of the last nine amino acid residues (Kim *et al.*, 2016). The presence of
324 a cysteine at the last position of BnaFT.C6 instead of the threonine of BnaFT.A7 alters
325 biochemical properties and could cause covalent protein-protein cross-linking under oxidizing
326 conditions (Figure 2D). Modified protein versions carrying a mutual exchange of the last
327 residue (BnaFT.A7m and BnaFT.C6m) were expressed in *ft-10* under the control of *C+A-FTp*.
328 T1 plants transformed with *BnaFT.A7m* showed a significant delay in flowering compared to
329 *BnaFT.A7* transformed lines (Figure 2E). In contrast, *BnaFT.C6m* T1 plants did not flower
330 earlier than *BnaFT.C6* transformed plants (Figure 2E). Taken together, the data indicate that a
331 cysteine as the last amino-acid contributed to a reduced florigen function of BnaFT.C6, but was
332 not the only determinant. Comparison of BnaFT.C6 from different cultivars revealed that the
333 threonine to cysteine change at the last amino-acid position was only found in a subset of semi-
334 winter cultivars (Supplemental Figure 4).

335 **Expression of *FT* homologs across tissues**
336 Although *BnaFT.C6*, *BnaNFT.A7* and *BnaCFT.C4* may not encode fully functional mobile
337 florigens, they induce flowering if transcribed close to the apical meristem. We compared

338 steady-state mRNA levels of *BnaFT*-like genes in different tissues and developmental stages in
339 the cultivar ZS11 grown in LD with and without vernalization (Figure 3). Our RT-qPCR
340 protocol used genomic DNA as a common reference point to allow copy-number comparisons
341 of mRNA levels between homologs. Without vernalization, no differences in steady-state
342 mRNA levels were detected between leaf 6 and leaf 8. In the case of vernalized plants, leaf 6
343 was fully expanded before while leaf 8 expanded after the plants were moved to and out of the
344 vernalization chamber, respectively. *BnaFT.A7* and *BnaFT.C6* were strongly induced in leaf 8
345 of vernalized compared to non-vernalized plants, while *BnaFT.A2* was vernalization-responsive
346 but less induced. As previously reported, *BnaFT.C2* was barely expressed, which has been
347 attributed to the presence of several TE insertions at the locus (Wang *et al.*, 2012a). After
348 vernalization, *BnaFT.A2* was expressed at much lower levels than *BnaFT.A7*/*BnaFT.C6* in leaf
349 8, but became the highest expressed *FT*-like gene in paraclade leaves. Steady-state mRNA
350 levels were similar for all three *FT* orthologs in floral buds, flowers and developing siliques. In
351 contrast, expression of *BnaFT.C2, BnaNFT.A7* and *BnaCFT.C4* was low throughout
352 development; therefore, these *FT*-like genes are unlikely to play a major regulatory role for
353 flowering regulation or inflorescence development under our test conditions.

354 **Conservation of cis-regulatory regions at *B. napus FT* homologs**

355 Previous reports established that the distal *FT* enhancer Block C is conserved at *FT* orthologs
356 between *B. napus* and *A. thaliana* (Adrian *et al.*, 2010; Wang *et al.*, 2012a). Here we show that
357 this is also the case for Block E, which is located downstream of the structural gene. *FT*
358 orthologs of *B. oleracea*, *B. rapa* and *S. parvula* showed the presence of all three blocks, while
359 non-orthologous *FT* homologues showed no conservation of the distal blocks and limited
360 conservation at the proximal promoter Block A (Supplementary Figure 5).
361 In *A. thaliana*, *FT* transcription is dependent on the NF-Y/CO-complex, but also requires
362 canonical NF-Y complexes, that contain NF-YA family proteins instead of CO (Wenkel *et al.*,
363 2006; Kumimoto *et al.*, 2008, 2010; Siriwardana *et al.*, 2016). The effect of NF-Y is likely mediated
364 by cognate CCAAT-boxes located at the distal enhancers Block C and Block E (Cao *et al.*, 2014;
365 Siriwardana *et al.*, 2016; Zicola *et al.*, 2019). A CCACA-motif as high-affinity binding site of the
366 CO-complex is found three times at Block A; a CCACT-motif that still binds the CO-complex
367 with fair affinity is found twice (Gnesutta *et al.*, 2017) (Figure 4A). The function of three distinct
368 CCACA-motifs, named P1, P2 and CORE2, has been experimentally validated (Adrian *et al.*,
369 2010; Tiwari *et al.*, 2010). In *B. napus*, CO-binding motifs P2 and CORE2 are present at
370 *BnaFT.A2/BnaFT.C2,* P1 is present as CCACT-motif in *BnaFT.A7*, *BnaFT.A2*, *BnaFT.C2* and
371 *SpFT*, while an additional C to A change creates a CCAAT-motif at the same position in

372 *BnaFT.C6*. A second change from CCACT- to CCAAT-motif is common to *BnaFT.C6*,
373 *BnaFT.A7* and *SpFT*. *BnaFT.C6* contains a third, private CCAAT-motif close to the
374 transcription start site. A recent structural study of the CO-complex with target DNA indicated
375 that only the CACA core of the first motif was involved in protein-DNA interactions (Lv *et al.*,
376 2021). Two additional CACA-motifs can be identified at Block A of which one is present in all
377 *BnaFT* paralogs and *SpFT*. In sum, more CO-binding CCACA-motifs are observed in block A
378 in a trend from *BnaFT.C6* to *BnaFT.A7*, *SpFT*, *BnaFT.A2/BnaFT.C2* and *FT*, while a trend
379 towards more NF-Y-binding CCAAT-motifs is observed in the opposite order. Notably, trend
380 to more promoter-located CCAAT-motifs correlated with expression levels in leaves.
381 At Block C, an important CCAAT-motif is conserved in all *FT* orthologs (Figure 4B), but at
382 the downstream enhancer Block E, *SpFT*, *BnaFT.C6* and *BnaFT.A7* share a CCACA-motif that
383 is not present at the other genes; furthermore, *BnaFTA7* and *BnaFTC6* have evolved two
384 additional CCACA sites as candidates for binding a CO-complex (Figure 4C). In contrast, the
385 first CCAAT motif has been lost at these homeologs.
386 To test whether the variation in *cis*-motifs at *B. napus FT* promoters had an impact on gene
387 activation by CO, we cloned upstream sequence of *FT* and *B. napus* orthologs to a binary
388 Luciferase reporter vector that allowed us to test transactivation by *B. napus* CO homologs in
389 transiently infiltrated tobacco leaves. The distance between regulatory blocks differs greatly in
390 *B.napus* and we could not amplify the 21 Kb promoter region of *BnaFT.C2* (Figure 4D). We
391 tested *BnaFT.A7*, *BnaFT.C6*, *BnaFT.A2* and *FT* promoter-mediated reporter gene induction in
392 response to BnaCO.A10 and BnaCO.9 controlled by the *CaMV 35S* promoter. We found that
393 promoters of *FT* and *BnaFT.A2* could be activated in the presence of both *B. napus* COs while
394 the homeolog pair *BnaFT.A7/BnaFT.C6* was not or significantly less induced (Figure 4E).
395 In sum, *BnaFT.A2*, which shows conservation of putative CO binding CCACA-motifs at the
396 proximal promoter is responsive to *B. napus* CO homologs in transient assays. In contrast,
397 homeologs *BnaFT.A7/BnaFT.C6* respond poorly to transactivation, corresponding to the
398 absence of conserved CO- binding motifs at the promoter.

399 **Diurnal expression pattern of *B. napus FT* homologs in response to photoperiod and**
400 **vernalization**

401 Since the homeologs Bna*FT.A2/BnaFT.C2* and *BnaFT.A7/BnaFT.C6* showed remarkable
402 differences in the distribution of cis motifs across regulatory blocks, we compared their
403 transcript levels across time-series of plants grown in SD and LD photoperiod both before and
404 after vernalization. The analysis confirmed that *BnaFT.A2*, *BnaFT.A7* and *BnaFT.C6* respond
405 to vernalization; furthermore, expression was induced by LD versus SD conditions, with a

406 strong synergism between LD and vernalization signals (Figure 5). The expression of
407 *BnaFT.C2* was low (approximately 20 and 100 times less than *BnaFT.A2* and *BnaFT.C6,*
408 respectively) but essentially followed the same induction pattern. In the case of non-*FT*
409 orthologs, *BnaCFT.C4* mirrored the vernalization response and the diurnal expression pattern
410 of *BnaFT* genes, at a level 10 times lower than *BnaFT.C2*. *BnaNFT.A7* was only notably
411 expressed at the beginning of LDs before vernalization. Overall, apart from *BnaNFT.A7*, *FT*-
412 like genes shared an expression minimum at ZT8 and high expression throughout the night until
413 the next morning (Figure 5 A and B).

414 **Photoperiod-dependent regulation of putative *B. napus* *FT* activators**

415 Differences in the arrangement of cis-motif for NF-Y/CO- and NF-Y complexes between
416 regulatory regions did not abolish the dependence of *BnaFT* genes on LD photoperiod. In *A.*
417 *thaliana*, the accumulation of CO protein in the second half of long days largely explains LD
418 dependency of *FT* expression, but it is not yet addressed if this model applies to other
419 Brassicaceae. We measured steady-state transcript levels of *BnaCO.A10* and *BnaCO.C9* in
420 leaves throughout SD and LDs before and after vernalization (Figure 5C). As previously
421 described, *BnaCO.C9* mRNA accumulated at higher levels than *BnaCO.A10* (Jin *et al.*, 2021b).
422 Both genes showed higher expression in LD vs SD, with similar trends before and after
423 vernalization. As observed for *BnaFT*-like genes, transcript levels of both *BnaCO* genes showed
424 a trough at ZT8 in LD. For *BnaCO.A10,* the general pattern of transcript accumulation was
425 similar in SD and LD, showing an increase during the dark and at dawn. For *BnaCO.C9*, steady-
426 state levels declined 8 h after the onset of the dark period in SD corresponding to the onset of
427 dark in LD, but transcript levels continued to increase in LD during the dark period. Under the
428 assumption that CO proteins in *B. napus* require light for stabilization, only *BnaCO.A10*
429 transcripts accumulating in the morning would contribute to a NF-Y/CO complex in the
430 morning in SD, while both COs could contribute to early morning and late afternoon NF-Y/CO
431 complexes in LD.

432 To assess whether NF-Y components could also limit *FT* gene expression in *B. napus*, we
433 generated RNAseq libraries of a diurnal time-series of vernalized ZS11 plants grown in LD and
434 SD photoperiod. Of the annotated 95560 nuclear *B. napus* genes, 47198 were considered as
435 expressed (at least 25 transcripts per million (TPM) summed across all samples) (Supplemental
436 Data 2). After applying the Rhythmicity Analysis Incorporating non-Parametric methods
437 (RAIN) pipeline with a FDR <0.05, 33714 genes (71,4%) scored as diurnally expressed, with
438 a slightly higher number in SD vs LD (29596 vs 21757). Most genes were detected as diurnally

439 expressed in both photoperiods (52.3%), but more genes were SD- than LD-specific (35.5% vs
440 12.2%, respectively) (Figure 6A, Supplemental Data 3).
441 We re-annotated *B. napus* NF-Y genes based on synteny to *A. thaliana* homologs and removed
442 four genes that were annotated as NF-Y genes but that likely encoded by pseudogenes due to a
443 partial protein prediction and/or frame-shift mutations (Supplemental Table 4, Supplemental
444 Figure 6). We found that 78 of 106 NF-Y genes were expressed, of which 55 showed diurnal
445 changes in their transcript levels. The fraction of diurnally expressed NF-Y genes is as expected
446 and although a slightly greater than expected number of NF-Y genes showed LD-specific
447 rhythmicity, this was not statistically significant (Figure 6B). Hierarchical clustering of
448 diurnally expressed *B. napus* NF-Y genes based on their transcript accumulation patterns
449 (normalized across all samples) identified 3 major clades (Figure 6C). A clade containing 29
450 NF-Y genes was expressed at higher level in LD versus SD and showed a marked peak of
451 expression in the critical afternoon light period from ZT12 to ZT16 in LD. The clade also
452 included *BnaFT* and CO genes that had been added to the clustering analysis; however,
453 expression of these genes extended to the dark phase and/or showed later peak values than
454 ZT16.
455 In *A. thaliana*, NF-Y paralogs with a critical role in *FT* expression were identified by their
456 phloem-specific expression and subsequently tested by reverse genetic approaches (Kumimoto
457 *et al.*, 2008, 2010; Siriwardana *et al.*, 2016). Although the tissue-specific expression pattern of NF-
458 Y genes in *B. napus* is unknown, it is noteworthy that 4 of 4 NF-YB2 homologs, 4 of 5 NF-
459 YC9 homologs and 2 of 3 NF-YA2 homologs, all orthologs of photoperiod-responsive NF-Ys,
460 are part of the expression cluster with an LD-specific peak at ZT16. *B. napus* homeologs are
461 likely to act redundantly and we therefore prepared cumulative plots that consider the
462 expression of all *B. napus* NF-YB2, NF-YC9 and NF-YA2 genes (Figure 6 D-F). If the sum of
463 the expression of all homeologs is considered, a marked peak of expression at ZT16 in LD and
464 an overall higher expression in LD vs SD was detected. In sum, NF-Y genes that are candidates
465 for photoperiod-dependent induction of *FT*-like genes could strongly promote *FT* expression at
466 the end of LD.

# 467 Discussion

468 Land plants share a recurrent history of whole genome duplications (WGD) through
469 polyploidisation and subsequent retraction of the coding genome (Panchy *et al.*, 2016). In some
470 cases, homeologs may be retained if increased gene dosage of redundant genes confers a fitness
471 advantage, but more often retention is linked to partial redundancy either through the evolution

472 of divergent expression patterns or through preferred interactions with other protein partners.
473 *B. napus* is a particularly rewarding case for study, combining two paleontological events with
474 different outcomes with a recent hybridisation event that has been partially shaped by human
475 selection for crop traits (Parkin *et al.*, 2005; Lu *et al.*, 2019).
476 Analysis of the genome of the genus Brassica suggests that one of the paleo-duplications
477 resulted in unequal retention of homeologs, while for the second event, two fairly co-linear
478 genomes can still be recognized (Parkin *et al.*, 2005). Only two *FT* syntenic genes are conserved
479 per Brassica genome lineage, indicating a loss of the copy of the weaker genome from the first
480 polyploidisation event. *NFT* and *CFT* are not survivors of the weak genome as syntenic copies
481 can be detected in *S. paruvula,* a sister genus of *Brassica* that did not undergo whole genome
482 duplication (Figure 1) (Cheng *et al.*, 2012). Differences in expression may have contributed to the
483 maintenance of both *FT* paralogs. In the case of the Brassica A genome, both paralogs are
484 expressed; however, expression seems specialised as *BnaFT.A7* and *BnaFT.A2* show higher
485 expression in rosette and paraclade leaves, respectively (Figure 3). In the case of the C-genome,
486 *BnaFT.C2* is barely expressed, probably due to the presence of TE insertions that are common
487 to *B. napus* but not to all *B. oleracea* varieties (Wang *et al.*, 2012a). Since *BnaFT.C2* encodes a
488 fully functional florigen (Figure 2), the presence of a second *FT*, even if only marginally
489 expressed, may be advantageous under certain conditions and therefore retained. Similarly,
490 circumstances causing the induction of *BnaNFT.C6* and *BnaCFT.C4* could influence flowering
491 and convey an advantage; however, *BnaNFT.C6* homeologs have not survived as functional
492 genes (Figure 1). Similarly, *BnaFT.C6*, the second *FT* of the C-genome may be impaired or at
493 least attenuated for its florigen function (Figure 2). The amino acid change from threonine to
494 cysteine, which contributed to the reduced systemic function, is not found in all *B. napus*
495 accessions (Supplemental Figure 4). Further studies are required to clarify whether the mutation
496 can be linked to a flowering QTL. In the case of the semi-winter *B. napus* variant ZS11, both
497 *FT* genes originating from the C-genome seem compromised in their function.
498 *A. thaliana FT* regulation depends on an intricate interplay of two distal enhancers with an
499 accessible chromatin structure and a proximal promoter that is inaccessible (Zicola *et al.*, 2019).
500 Binding of NF-Y complexes to distal enhancers is thought to somehow increase the probability
501 of NF-Y/CO to bind to the proximal promoter and increase expression; how NF-Y/CO binding
502 is mechanistically linked the induction of transcription is currently unknown. Although the cis-
503 regulatory Blocks were found as conserved at all *B. napus FT* genes, the shift from NF-Y/CO
504 to NF-Y binding sites at the proximal promoter was unexpected and raises a couple of questions
505 (Figure 4). First, can binding of NF-Y simply replace NF-Y/CO causing similar effects leading

506 to the induction of transcripts? Second, if NF-Y binding is sufficient to induce expression, what
507 limits induction of BnaFTA7/BnaFTC6 to LD? Here, we propose that transcriptional regulation
508 of NF-Y genes may contribute to photoperiod control (Figure 6). Alternatively, *B.napus* CO
509 proteins as part of a NF-Y/CO complex binding to the distal enhancer could contribute as
510 limiting factors, but how it could do so is not obvious. Gnesutta et al. determined the binding
511 preferences of the NF-Y/CO complex to DNA (Gnesutta *et al.*, 2017). The preferred binding motif
512 for NF-Y/CO (CCACA) is two nucleotide edits away from the CCAAT motif. We found that
513 replacement of motifs happened at conserved in the proximal promoter and propose that an
514 intermediate CCACT motif that can still be bound (or already be bound) by NF-Y/CO served
515 as stepping stone during the motif change (Figure 4).
516 In sum, *B. napus* photoperiod dependent regulation of *FT*-like genes is a case study for the
517 consequence of gene duplications, indicating gene retraction through loss-of-function,
518 homeolog retention partially explained by differences transcriptional regulation and possibly
519 variation between cultivated varieties due to changes in protein function.
520

521 # Acknowledgements

522 JW is grateful for the funding from the Chinese Scholarship Council. FT and HZ are supported
523 by core funding from the Max Planck Society.

524 # Competing interests

525 None declared.

526 # Author contributions

527 JJW and FT outlined, created figures and wrote the manuscript outline. JJW performed all
528 experimental work, FT and HRZ contributed with guidance and critical discussion. JJW and FT
529 performed all data analysis. JJW, FT, HRZ and JW were involved in revising the manuscript.

530 # Data availability

531 RNAseq datasets generated and analysed in the current study are available at the European
532 Nucleotide archive under the accession number project accession number PRJEB82128.

533 # References


534 **Abe M, Kobayashi Y, Yamamoto S, Daimon Y, Yamaguchi A, Ikeda Y, Ichinoki H,**
535 **Notaguchi M, Goto K, Araki T**. **2005**. FD, a bZIP protein mediating signals from the floral
536 pathway integrator FT at the shoot apex. *Science* **309**: 1052–1056.

537 **Adrian J, Farrona S, Reimer JJ, Albani MC, Coupland G, Turck F**. **2010**. cis-Regulatory
538 elements and chromatin state coordinately control temporal and spatial expression of
539 FLOWERING LOCUS T in Arabidopsis. *The Plant Cell* **22**: 1425–1440.

540 **Andrés F, Coupland G**. **2012**. The genetic basis of flowering responses to seasonal cues.
541 *Nature Reviews. Genetics* **13**: 627–639.

542 **Bratzel F, Turck F**. **2015**. Molecular memories in the regulation of seasonal flowering: from
543 competence to cessation. *Genome Biology* **16**: 192.

544 **Cao S, Kumimoto RW, Gnesutta N, Calogero AM, Mantovani R, Holt BF**. **2014**. A distal
545 CCAAT/NUCLEAR FACTOR Y complex promotes chromatin looping at the FLOWERING
546 LOCUS T promoter and regulates the timing of flowering in Arabidopsis. *The Plant Cell* **26**:
547 1009–1017.

548 **Chalhoub B**. **2014**. Early allopolyploid evolution in the post-Neolithic Brassica napus oilseed
549 genome (vol 348, 1260782, 2014). *Science* **345**: 1255–1255.

550 **Cheng F, Mandáková T, Wu J, Xie Q, Lysak MA, Wang X**. **2013**. Deciphering the diploid
551 ancestral genome of the Mesohexaploid Brassica rapa. *The Plant Cell* **25**: 1541–1554.

552 **Cheng F, Wu J, Fang L, Wang X**. **2012**. Syntenic gene analysis between Brassica rapa and
553 other Brassicaceae species. *Frontiers in Plant Science* **3**: 198.

554 **Clough SJ, Bent AF**. **1998**. Floral dip: a simplified method for *Agrobacterium*-mediated
555 transformation of *Arabidopsis thaliana*. *The Plant Journal* **16**: 735–743.

556 **Dobin A, Davis CA, Schlesinger F, Drenkow J, Zaleski C, Jha S, Batut P, Chaisson M,**
557 **Gingeras TR**. **2013**. STAR: ultrafast universal RNA-seq aligner. *Bioinformatics* **29**: 15–21.

558 **Endo M, Yoshida M, Sasaki Y, Negishi K, Horikawa K, Daimon Y, Kurotani K-I,**
559 **Notaguchi M, Abe M, Araki T**. **2018**. Re-Evaluation of Florigen Transport Kinetics with
560 Separation of Functions by Mutations That Uncouple Flowering Initiation and Long-Distance
561 Transport. *Plant & Cell Physiology* **59**: 1621–1629.

562 **Fernández V, Takahashi Y, Le Gourrierec J, Coupland G**. **2016**. Photoperiodic and
563 thermosensory pathways interact through CONSTANS to promote flowering at high
564 temperature under short days. *The Plant Journal* **86**: 426–440.

565 **Fornara F, Panigrahi KCS, Gissot L, Sauerbrunn N, Rühl M, Jarillo JA, Coupland G**.
566 **2009**. Arabidopsis DOF transcription factors act redundantly to reduce CONSTANS
567 expression and are essential for a photoperiodic flowering response. *Developmental Cell* **17**:
568 75–86.

569 **Galvão VC, Fiorucci A-S, Trevisan M, Franco-Zorilla JM, Goyal A, Schmid-Siegert E,**
570 **Solano R, Fankhauser C**. **2019**. PIF transcription factors link a neighbor threat cue to
571 accelerated reproduction in Arabidopsis. *Nature Communications* **10**: 4005.

572 **Gnesutta N, Kumimoto RW, Swain S, Chiara M, Siriwardana C, Horner DS, Holt BF,**
573 **Mantovani R**. **2017**. CONSTANS Imparts DNA Sequence Specificity to the Histone Fold
574 NF-YB/NF-YC Dimer. *The Plant Cell* **29**: 1516–1532.

575 **Guo Y, Hans H, Christian J, Molina C**. **2014**. Mutations in single FT- and TFL1-paralogs
576 of rapeseed (Brassica napus L.) and their impact on flowering time and yield components.
577 *Frontiers in Plant Science* **5**: 282.

578 **Hatje K, Keller O, Hammesfahr B, Pillmann H, Waack S, Kollmar M**. **2011**. Cross-
579 species protein sequence and gene structure prediction with fine-tuned Webscipio 2.0 and
580 Scipio. *BMC Research Notes* **4**: 265.

581 **Imaizumi T, Schultz TF, Harmon FG, Ho LA, Kay SA**. **2005**. FKF1 F-box protein
582 mediates cyclic degradation of a repressor of CONSTANS in Arabidopsis. *Science* **309**: 293–
583 297.

584 **Jaeger KE, Wigge PA**. **2007**. FT protein acts as a long-range signal in Arabidopsis. *Current*
585 *Biology* **17**: 1050–1054.

586 **Jang S, Marchal V, Panigrahi KCS, Wenkel S, Soppe W, Deng X-W, Valverde F,**
587 **Coupland G**. **2008**. Arabidopsis COP1 shapes the temporal pattern of CO accumulation
588 conferring a photoperiodic flowering response. *The EMBO Journal* **27**: 1277–1288.

589 **Jin Q, Gao G, Guo C, Yang T, Li G, Song J, Zheng N, Yin S, Yi L, Li Z, *et al.* 2022**.
590 Transposon insertions within alleles of BnaFT.A2 are associated with seasonal crop type in
591 rapeseed. *TAG. Theoretical and Applied Genetics. Theoretische und Angewandte Genetik*
592 **135**: 3469–3483.

593 **Jin S, Nasim Z, Susila H, Ahn JH**. **2021a**. Evolution and functional diversification of
594 FLOWERING LOCUS T/TERMINAL FLOWER 1 family genes in plants. *Seminars in Cell*
595 *& Developmental Biology* **109**: 20–30.

596 **Jin Q, Yin S, Li G, Guo T, Wan M, Li H, Li J, Ge X, King GJ, Li Z, *et al.* 2021b**.
597 Functional homoeologous alleles of CONSTANS contribute to seasonal crop type in
598 rapeseed. *TAG. Theoretical and Applied Genetics. Theoretische und Angewandte Genetik*
599 **134**: 3287–3303.

600 **Kagale S, Robinson SJ, Nixon J, Xiao R, Huebert T, Condie J, Kessler D, Clarke WE,**
601 **Edger PP, Links MG, *et al.* 2014**. Polyploid evolution of the Brassicaceae during the
602 Cenozoic era. *The Plant Cell* **26**: 2777–2791.

603 **Kiełbasa SM, Wan R, Sato K, Horton P, Frith MC**. **2011**. Adaptive seeds tame genomic
604 sequence comparison. *Genome Research* **21**: 487–493.

605 **Kim S-J, Hong SM, Yoo SJ, Moon S, Jung HS, Ahn JH**. **2016**. Post-Translational
606 Regulation of FLOWERING LOCUS T Protein in Arabidopsis. *Molecular Plant* **9**: 308–311.

607 **Kumar SV, Lucyshyn D, Jaeger KE, Alós E, Alvey E, Harberd NP, Wigge PA**. **2012**.
608 Transcription factor PIF4 controls the thermosensory activation of flowering. *Nature* **484**:
609 242–245.

610 **Kumimoto RW, Adam L, Hymus GJ, Repetti PP, Reuber TL, Marion CM, Hempel FD,**
611 **Ratcliffe OJ**. **2008**. The Nuclear Factor Y subunits NF-YB2 and NF-YB3 play additive roles
612 in the promotion of flowering by inductive long-day photoperiods in Arabidopsis. *Planta* **228**:
613 709–723.

614 **Kumimoto RW, Zhang Y, Siefers N, Holt BF**. **2010**. NF-YC3, NF-YC4 and NF-YC9 are
615 required for CONSTANS-mediated, photoperiod-dependent flowering in Arabidopsis
616 thaliana. *The Plant Journal* **63**: 379–391.

617 **Laubinger S, Marchal V, Le Gourrierec J, Wenkel S, Adrian J, Jang S, Kulajta C,**
618 **Braun H, Coupland G, Hoecker U**. **2006**. Arabidopsis SPA proteins regulate photoperiodic
619 flowering and interact with the floral inducer CONSTANS to regulate its stability.
620 *Development* **133**: 3213–3222.

621 **Li B, Dewey CN**. **2011**. RSEM: accurate transcript quantification from RNA-Seq data with or
622 without a reference genome. *BMC Bioinformatics* **12**: 323.

623 **Liu L, Adrian J, Pankin A, Hu J, Dong X, von Korff M, Turck F**. **2014**. Induced and
624 natural variation of promoter length modulates the photoperiodic response of FLOWERING
625 LOCUS T. *Nature Communications* **5**: 4558.

626 **Liu Y, Li X, Li K, Liu H, Lin C**. **2013**. Multiple bHLH proteins form heterodimers to
627 mediate CRY2-dependent regulation of flowering-time in Arabidopsis. *PLoS Genetics* **9**:
628 e1003861.

629 **Liu Y, Li X, Ma D, Chen Z, Wang J-W, Liu H**. **2018**. CIB1 and CO interact to mediate
630 CRY2-dependent regulation of flowering. *EMBO Reports* **19**.

631 **Lu K, Wei L, Li X, Wang Y, Wu J, Liu M, Zhang C, Chen Z, Xiao Z, Jian H, *et al.* 2019**.
632 Whole-genome resequencing reveals Brassica napus origin and genetic loci involved in its
633 improvement. *Nature Communications* **10**: 1154.

634 **Lv X, Zeng X, Hu H, Chen L, Zhang F, Liu R, Liu Y, Zhou X, Wang C, Wu Z, *et al.***
635 **2021**. Structural insights into the multivalent binding of the Arabidopsis FLOWERING
636 LOCUS T promoter by the CO-NF-Y master transcription factor complex. *The Plant Cell* **33**:
637 1182–1195.

638 **Panchy N, Lehti-Shiu M, Shiu S-H**. **2016**. Evolution of gene duplication in plants. *Plant*
639 *Physiology* **171**: 2294–2316.

640 **Parkin IAP, Gulden SM, Sharpe AG, Lukens L, Trick M, Osborn TC, Lydiate DJ**. **2005**.
641 Segmental structure of the Brassica napus genome based on comparative analysis with
642 Arabidopsis thaliana. *Genetics* **171**: 765–781.

643 **Pin PA, Benlloch R, Bonnet D, Wremerth-Weich E, Kraft T, Gielen JJL, Nilsson O**.
644 **2010**. An antagonistic pair of FT homologs mediates the control of flowering time in sugar
645 beet. *Science* **330**: 1397–1400.

646 **Posé D, Verhage L, Ott F, Yant L, Mathieu J, Angenent GC, Immink RGH, Schmid M**.
647 **2013**. Temperature-dependent regulation of flowering by antagonistic FLM variants. *Nature*
648 **503**: 414–417.

649 **Sawa M, Nusinow DA, Kay SA, Imaizumi T**. **2007**. FKF1 and GIGANTEA complex
650 formation is required for day-length measurement in Arabidopsis. *Science* **318**: 261–265.

651 **Schiessl S, Samans B, Hüttel B, Reinhard R, Snowdon RJ**. **2014**. Capturing sequence
652 variation among flowering-time regulatory gene homologs in the allopolyploid crop species
653 Brassica napus. *Frontiers in Plant Science* **5**: 404.

654 **Schiessl S**. **2020**. Regulation and Subfunctionalization of Flowering Time Genes in the
655 Allotetraploid Oil Crop Brassica napus. *Frontiers in Plant Science* **11**: 605155.

656 **Siriwardana CL, Gnesutta N, Kumimoto RW, Jones DS, Myers ZA, Mantovani R, Holt**
657 **BF**. **2016**. NUCLEAR FACTOR Y, Subunit A (NF-YA) Proteins Positively Regulate
658 Flowering and Act Through FLOWERING LOCUS T. *PLoS Genetics* **12**: e1006496.

659 **Song J-M, Guan Z, Hu J, Guo C, Yang Z, Wang S, Liu D, Wang B, Lu S, Zhou R, *et al.***
660 **2020**. Eight high-quality genomes reveal pan-genome architecture and ecotype differentiation
661 of Brassica napus. *Nature Plants* **6**: 34–45.

662 **Sparkes IA, Runions J, Kearns A, Hawes C**. **2006**. Rapid, transient expression of
663 fluorescent fusion proteins in tobacco plants and generation of stably transformed plants.
664 *Nature Protocols* **1**: 2019–2025.

665 **Takagi H, Hempton AK, Imaizumi T**. **2023**. Photoperiodic flowering in Arabidopsis:
666 Multilayered regulatory mechanisms of CONSTANS and the florigen FLOWERING LOCUS
667 T. *Plant communications* **4**: 100552.

668 **Tamura K, Stecher G, Kumar S**. **2021**. MEGA11: Molecular Evolutionary Genetics
669 Analysis version 11. *Molecular Biology and Evolution* **38**: 3022–3027.

670 **Tang H, Krishnakumar V, Zeng X, Xu Z, Taranto A, Lomas JS, Zhang Y, Huang Y,**
671 **Wang Y, Yim WC, *et al.* 2024**. JCVI: A versatile toolkit for comparative genomics analysis.
672 *iMeta* **3**: e211.

673 **Tang H, Wang X, Bowers JE, Ming R, Alam M, Paterson AH**. **2008**. Unraveling ancient
674 hexaploidy through multiply-aligned angiosperm gene maps. *Genome Research* **18**: 1944–
675 1954.

676 **Teotia S, Tang G**. **2015**. To bloom or not to bloom: role of microRNAs in plant flowering.
677 *Molecular Plant* **8**: 359–377.

678 **Thaben PF, Westermark PO**. **2014**. Detecting rhythms in time series with RAIN. *Journal of*
679 *Biological Rhythms* **29**: 391–400.

680 **Tiwari SB, Shen Y, Chang H-C, Hou Y, Harris A, Ma SF, McPartland M, Hymus GJ,**
681 **Adam L, Marion C, *et al.* 2010**. The flowering time regulator CONSTANS is recruited to the
682 FLOWERING LOCUS T promoter via a unique cis-element. *The New Phytologist* **187**: 57–
683 66.

**Valverde F, Mouradov A, Soppe W, Ravenscroft D, Samach A, Coupland G. 2004**. Photoreceptor regulation of CONSTANS protein in photoperiodic flowering. *Science* **303**: 1003–1006.

**Wang J, Hopkins CJ, Hou J, Zou X, Wang C, Long Y, Kurup S, King GJ, Meng J. 2012a**. Promoter variation and transcript divergence in Brassicaceae lineages of FLOWERING LOCUS T. *Plos One* **7**: e47127.

**Wang J, Long Y, Wu B, Liu J, Jiang C, Shi L, Zhao J, King GJ, Meng J. 2009**. The evolution of Brassica napus FLOWERING LOCUS T paralogues in the context of inverted chromosomal duplication blocks. *BMC Evolutionary Biology* **9**: 271.

**Wang Y, Tang H, Debarry JD, Tan X, Li J, Wang X, Lee T, Jin H, Marler B, Guo H, *et al.* 2012b**. MCScanX: a toolkit for detection and evolutionary analysis of gene synteny and collinearity. *Nucleic Acids Research* **40**: e49.

**Wenkel S, Turck F, Singer K, Gissot L, Le Gourrierec J, Samach A, Coupland G. 2006**. CONSTANS and the CCAAT box binding complex share a functionally important domain and interact to regulate flowering of Arabidopsis. *The Plant Cell* **18**: 2971–2984.

**Wigge PA, Kim MC, Jaeger KE, Busch W, Schmid M, Lohmann JU, Weigel D. 2005**. Integration of spatial and temporal information during floral induction in Arabidopsis. *Science* **309**: 1056–1059.

**Wu D, Liang Z, Yan T, Xu Y, Xuan L, Tang J, Zhou G, Lohwasser U, Hua S, Wang H, *et al.* 2019**. Whole-Genome Resequencing of a Worldwide Collection of Rapeseed Accessions Reveals the Genetic Basis of Ecotype Divergence. *Molecular Plant* **12**: 30–43.

**Yamaguchi A, Kobayashi Y, Goto K, Abe M, Araki T. 2005**. TWIN SISTER OF FT (TSF) acts as a floral pathway integrator redundantly with FT. *Plant & Cell Physiology* **46**: 1175–1189.

**Yanovsky MJ, Kay SA. 2002**. Molecular basis of seasonal time measurement in Arabidopsis. *Nature* **419**: 308–312.

**Yoo S-C, Chen C, Rojas M, Daimon Y, Ham B-K, Araki T, Lucas WJ. 2013**. Phloem long-distance delivery of FLOWERING LOCUS T (FT) to the apex. *The Plant Journal* **75**: 456–468.

**Zicola J, Liu L, Tänzler P, Turck F. 2019**. Targeted DNA methylation represses two enhancers of FLOWERING LOCUS T in Arabidopsis thaliana. *Nature Plants* **5**: 300–307.

**Zou J, Mao L, Qiu J, Wang M, Jia L, Wu D, He Z, Chen M, Shen Y, Shen E, *et al.* 2019**. Genome-wide selection footprints and deleterious variations in young Asian allotetraploid rapeseed. *Plant Biotechnology Journal* **17**: 1998–2010.

# Figure legends

**Figure 1. Phylogenetic and syntenic analysis of *FT* and *TSF* and their homologues in *B. napus*, *B. oleracea* and *S. parvula*.** (A)-(D) Microsynteny between *FT* homologs. *FT*-like genes from *A. thaliana* (bottom), *S. parvula* (middle) and *B. napus* (top) are connected by red lines, orthologs of flanking genes present in all genomes are connected by golden lines, orthologs of flanking genes that exist only in a subset of Brassica genomes are connected by purple, blue and gray lines. Genes are depicted as boxes (blue forward, green reverse orientation). **(A)** Four paralogous *FT* orthologs were identified in *B. napus*, one in *S. parvula*. **(B)** One *TSF* ortholog was identified in *S. parvula*, none in *B. napus*. **(C)** Three paralogous *FT*-like genes (*BnaNFT*) on Chr. A07/C02/C06 in *B. napus* have an ortholog in *S. parvula*, but not in *A. thaliana*. Only the paralogue on chromosome A07 (*BnaNFT.A7*) encodes a functional gene. **(D)** An *FT*-like gene on Chr. C04 (*BnaCFT.C4*) in *B. napus*, is present in the C-genome parent *B. oleracea* and absent in the *S. parvula* and *A. thaliana* genomes. (**E)** Full-length protein sequences of FT, TSF and FT homologues obtained by blast analysis against *B. napus*, *B. rapa*, *B. oleracea, A. lyrata* and *S. parvula* genomes were used to create the neighbour-joining (NJ) consensus tree using MEGA-11 with 1,000 bootstraps. TFL1, BFT, MFT were set as an outgroup, and FT and TSF orthologues in *A. thaliana* and *A. lyrata* were added for reference.

**Figure 2. Florigen function of *B. napus FT* homologs. (A)** Schematic illustration of the constructs used to complement *ft-10*. The *A. thaliana FD* promoter (*FD*p) or the synthetic *FT* promoter (*(C+A)-FTp*) was used to drive expression of *FT*, *BnaFTs*, *BnaNFT* and *BnaCFT* cDNA in *ft-10* plants in the shoot apical meristem and the *FT* expression domain in the phloem, respectively. **(B)** Flowering time of homozygous T3 plants of two representative *ft-10* lines transformed with *FT* and *B. napus FT* homologs driven by *(C+A)-FTp*. The number of plants used for analysis was greater or equal to 7. **(C)** Flowering time of independent T1 *ft-10* plants transformed with *FT* and *B. napus FT* homologs under the control of *FD*p. The number of T1 plants used for analysis was greater or equal to 13. **(D)** Selection of amino-acids alignment of *A. thaliana* and *B. napus FT* homologs. Arrows indicate differences between *BnaFT.A7* and *BnaFT.C6*. *BnaFT.A7m* and *BnaFT.C6m* are mutant versions in which the last amino acid residue was swapped. **(E)** Flowering time of independent T1 *ft-10* T1 plants transformed with *BnaFT.C6, BnaFT.A7, BnaFTC6m and BnaFTA7m* driven by *(C+A)-FTp*. The number of plants used for analysis was greater or equal to 13. (B, C, E) Flowering time was scored as total leaf number. Box plots show the medians as vertical lines; box limits indicate the 25th and 75th

751 percentiles. Different symbols from a to h above the plots indicate significant differences (P <
752 0.05, two-way analysis of variance (ANOVA) with Tukey's multiple comparison test).

753 **Figure 3. Tissue-specific expression of *B. napus FT* homologs in ZS11.** Expression of *B.*
754 *napus FT* homologs in roots, leaf 6, leaf 8, paraclade leaf, floral bud, flower and siliques. Plants
755 were sown in the greenhouse for 4 weeks under LD conditions, then vernalized for 4 weeks
756 before being transferred back to LD conditions in the greenhouse. Root and leaf 6 and 8 were
757 sampled before vernalization, leaf 8, paraclade leaf, floral bud, flower and siliques were
758 sampled after vernalization at ZT12. Boxes represent inner quartiles of three biological
759 replicates, medians are indicated by vertical lines, single measurements are indicated by dots.
760 *BnaENTH* was used as reference gene, all values were compared to genomic DNA, which was
761 set as 1.

762 **Figure 4. Conservation of the cis-regulatory code at *B. napus FT* homologs.**
763 Schematic diagram showing the distribution of motifs within conserved blocks A **(A)**, C **(B)**
764 and E **(C)** for *FT-like* genes from *A. thaliana, S. parvula* and *B. napus*. Gray boxes indicate
765 aligned sequences, white spaces indicate alignment gaps. Cis-elements are marked in different
766 colors as indicated in the common legend. The length of the unaligned sequences is shown after
767 each alignment block. Red numbers above the position of motifs at *FT* block A indicate
768 previously characterized functional motifs. (**D)** Scheme of the promoter region of *B. napus FT*
769 genes fused to LUC. (**E)** Promoter-reporter transactivation assay in infiltrated tobacco leaves.
770 Agrobacteria transformed with a binary vector containing promoter Firefly luciferase fusions
771 and Renilla luciferase under the control of the CaMV 35S promoter were co-infiltrated with
772 bacteria expressing either BnaCO.A10, BnaCO.C9 or an empty binary vector. Infiltrated areas
773 were extracted and Luciferase vs Renilla luciferase activity quantified. Boxplots show relative
774 firefly vs Renilla signal from 4 to 6 independent infiltrations, the median is indicated as line,
775 data-points as dots. Statistical analysis was performed using the non-parametric Wilcocxon
776 signed rank test with FDR correction.

777 **Figure 5. Diurnal expression of *B.* napus *FT* and *CO* homologs in ZS11. (A)** Diurnal
778 expression of *BnaFT.A2*, *BnaFT.C2*, *BnaFT.A7*, *BnaFT.C6*. **(B)** Diurnal expression of
779 *BnaNFT.A7* and *BnaCFT.C4.* (**C)** Diurnal expression of *BnaCO.A10* and *BnaCO.C9.* Material
780 from leaf 6 and leaf 8 were sampled every 4 h from ZS11 plants grown in SD and LD
781 photoperiod in growth chambers at 22°C before (BV) and after (AV) vernalization,
782 respectively. Time is plotted in reference to Zeitgeber (light on). Expression levels were
783 analysed by gene-specific qRT-PCR using four independent biological replicates using

784 genomic DNA as common reference point. *BnaENTH* was used to correct for differences in
785 cDNA amount. Values for ZT0 and ZT24 were pooled at both time points. Data points are
786 indicated as dots, lines were generated using a loess smoothing function, grey shapes indicate
787 ± standard error.

788 **Figure 6. Diurnal expression of *B.* napus NF-Y homologs. (A)** Venn diagram showing
789 rhythmically expressed genes in LD and SD photoperiod. (**B)** As A) for NF-Y genes. **(C)**
790 Heatmap of rhythmically expressed *B. napus* NF-Y genes after hierarchical clustering based on
791 expression patterns. Expression data in TPM were normalized across all samples per gene,
792 clustering was performed using the Manhattan distance metric. Colours indicate *B. napus*
793 homologs of *NF-Y*s involved in *FT* regulation (red), *BnaFT*s (blue) and *BnaCO*s (purple). (**D)**
794 Cumulative sum plot of TPM values in SD (left panel) and LD (right panel) for all *BnaNFYB2*
795 genes. (**E)** as D) for *BnaNF-YC9* genes. (**F)** as D) for *BnaNF-YA2* genes.

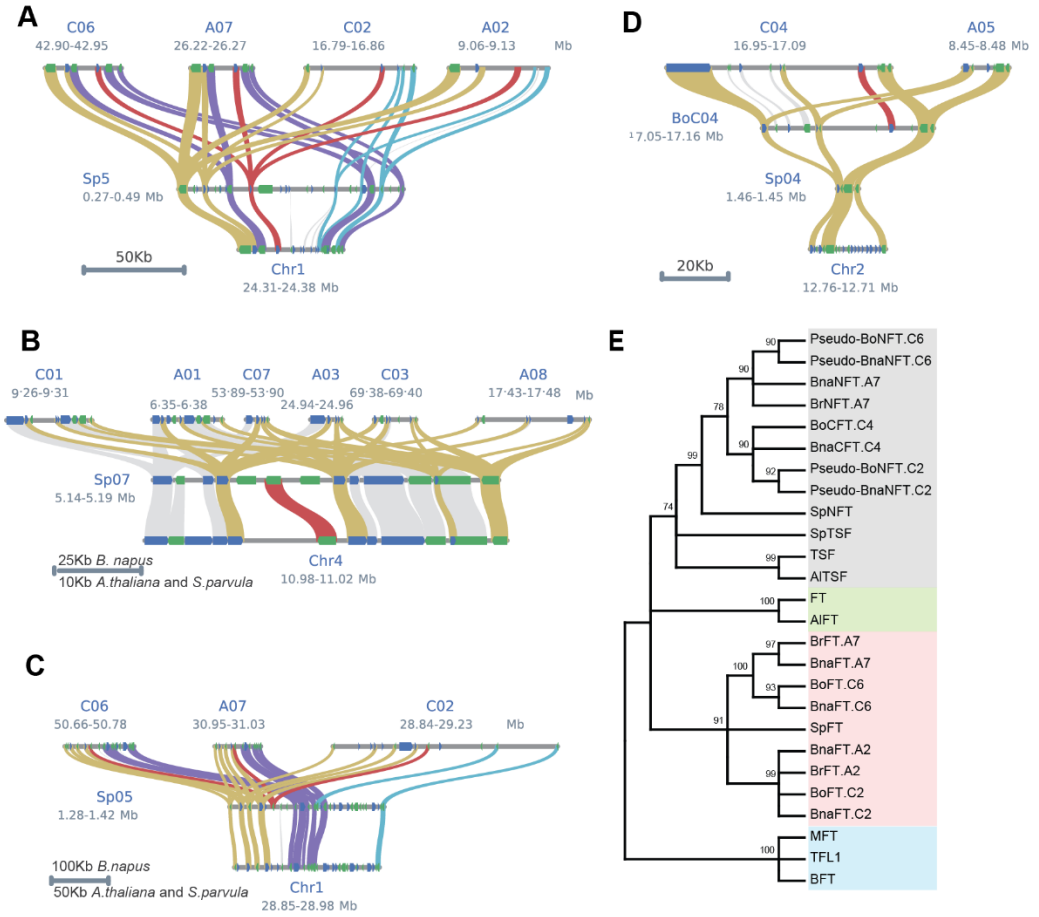


**Figure 1. Phylogenetic and syntenic analysis of *FT* and *TSF* and their homologues in *B. napus*, *B. oleracea* and *S. parvula*.** (A)-(D) Microsynteny between *FT* homologs. *FT*-like genes from *A. thaliana* (bottom), *S. parvula* (middle) and *B. napus* (top) are connected by red lines, orthologs of flanking genes present in all genomes are connected by golden lines, orthologs of flanking genes that exist only in a subset of Brassica genomes are connected by purple, blue and gray lines. Genes are depicted as boxes (blue forward, green reverse orientation). **(A)** Four paralogous *FT* orthologs were identified in *B. napus*, one in *S. parvula*. **(B)** One *TSF* ortholog was identified in *S. parvula*, none in *B. napus*. **(C)** Three paralogous *FT*-like genes (*BnaNFT*) on Chr. A07/C02/C06 in *B. napus* have an ortholog in *S. parvula*, but not in *A. thaliana*. Only the paralogue on chromosome A07 (*BnaNFT.A7*) encodes a functional gene. **(D)** An *FT*-like gene on Chr. C04 (*BnaCFT.C4*) in *B. napus*, is present in the C-genome parent *B. oleracea* and absent in the *S. parvula* and *A. thaliana* genomes. **(E)** Full-length protein sequences of FT, TSF and FT homologues obtained by blast analysis against *B. napus*, *B. rapa*, *B. oleracea, A. lyrata* and *S. parvula* genomes were used to create the neighbour-joining (NJ) consensus tree using MEGA-11 with 1,000 bootstraps. TFL1, BFT, MFT were set as an outgroup, and FT and TSF orthologues in *A. thaliana* and *A. lyrata* were added for reference.

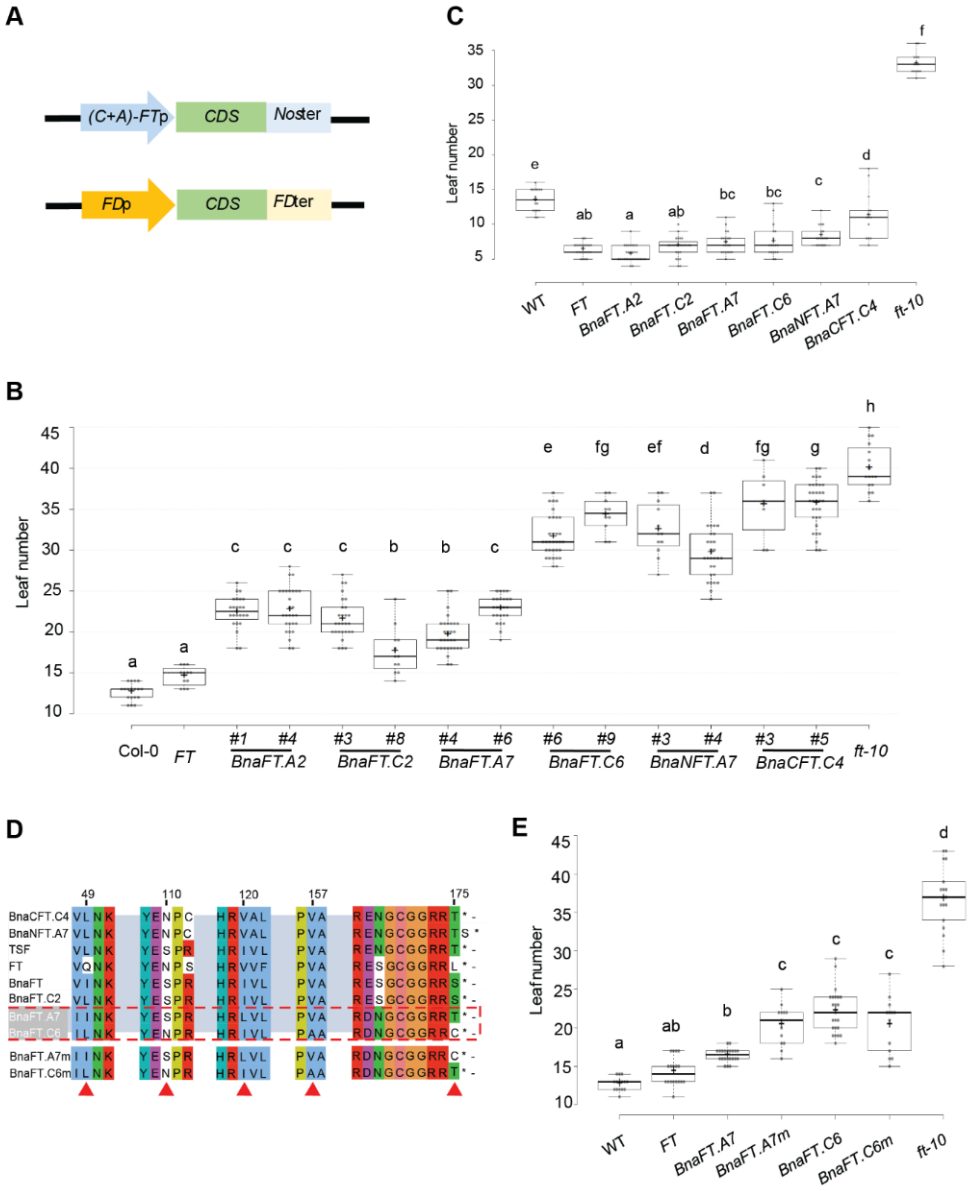


**Figure 2. Florigen function of *B. napus FT* homologs. (A)** Schematic illustration of the constructs used to complement *ft-10*. The *A. thaliana FD* promoter (*FD*p) or the synthetic *FT* promoter (*(C+A)-FTp*) was used to drive expression of *FT*, *BnaFTs*, *BnaNFT* and *BnaCFT* cDNA in *ft-10* plants in the shoot apical meristem and the *FT* expression domain in the phloem, respectively. **(B)** Flowering time of homozygous T3 plants of two representative *ft-10* lines transformed with *FT* and *B. napus FT* homologs driven by *(C+A)-FTp*. The number of plants used for analysis was greater or equal to 7. **(C)** Flowering time of independent T1 *ft-10* plants transformed with *FT* and *B. napus FT* homologs under the control of *FD*p. The number of T1 plants used for analysis was greater or equal to 13. **(D)** Selection of amino-acids alignment of *A. thaliana* and *B. napus FT* homologs. Arrows indicate differences between *BnaFT.A7* and *BnaFT.C6*. *BnaFT.A7m* and *BnaFT.C6m* are mutant versions in which the last amino acid residue was swapped. **(E)** Flowering time of independent T1 *ft-10* T1 plants transformed with *BnaFT.C6, BnaFT.A7, BnaFTC6m and BnaFTA7m* driven by *(C+A)-FTp*. The number of plants used for analysis was greater or equal to 13. (B, C, E) Flowering time was scored as total leaf number. Box plots show the medians as vertical lines; box limits indicate the 25th and 75th

829 percentiles. Different symbols from a to h above the plots indicate significant differences ($P <$
830 $0.05$, two-way analysis of variance (ANOVA) with Tukey's multiple comparison test).

831

832

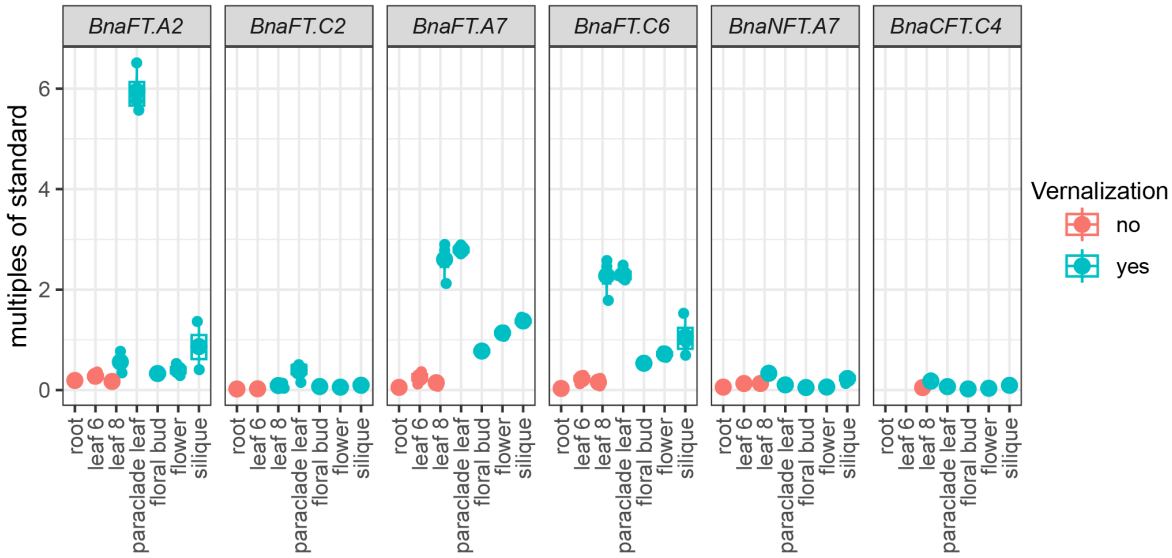


833

834 **Figure 3. Tissue-specific expression of *B. napus FT* homologs in ZS11.** Expression of *B.*
835 *napus FT* homologs in roots, leaf 6, leaf 8, paraclade leaf, floral bud, flower and siliques.
836 Plants were sown in the greenhouse for 4 weeks under LD conditions, then vernalized for 4
837 weeks before being transferred back to LD conditions in the greenhouse. Root and leaf 6 and
838 8 were sampled before vernalization, leaf 8, paraclade leaf, floral bud, flower and siliques
839 were sampled after vernalization at ZT12. Boxes represent inner quartiles of three biological
840 replicates, medians are indicated by vertical lines, single measurements are indicated by dots.
841 *BnaENTH* was used as reference gene, all values were compared to genomic DNA, which
842 was set as 1.

843

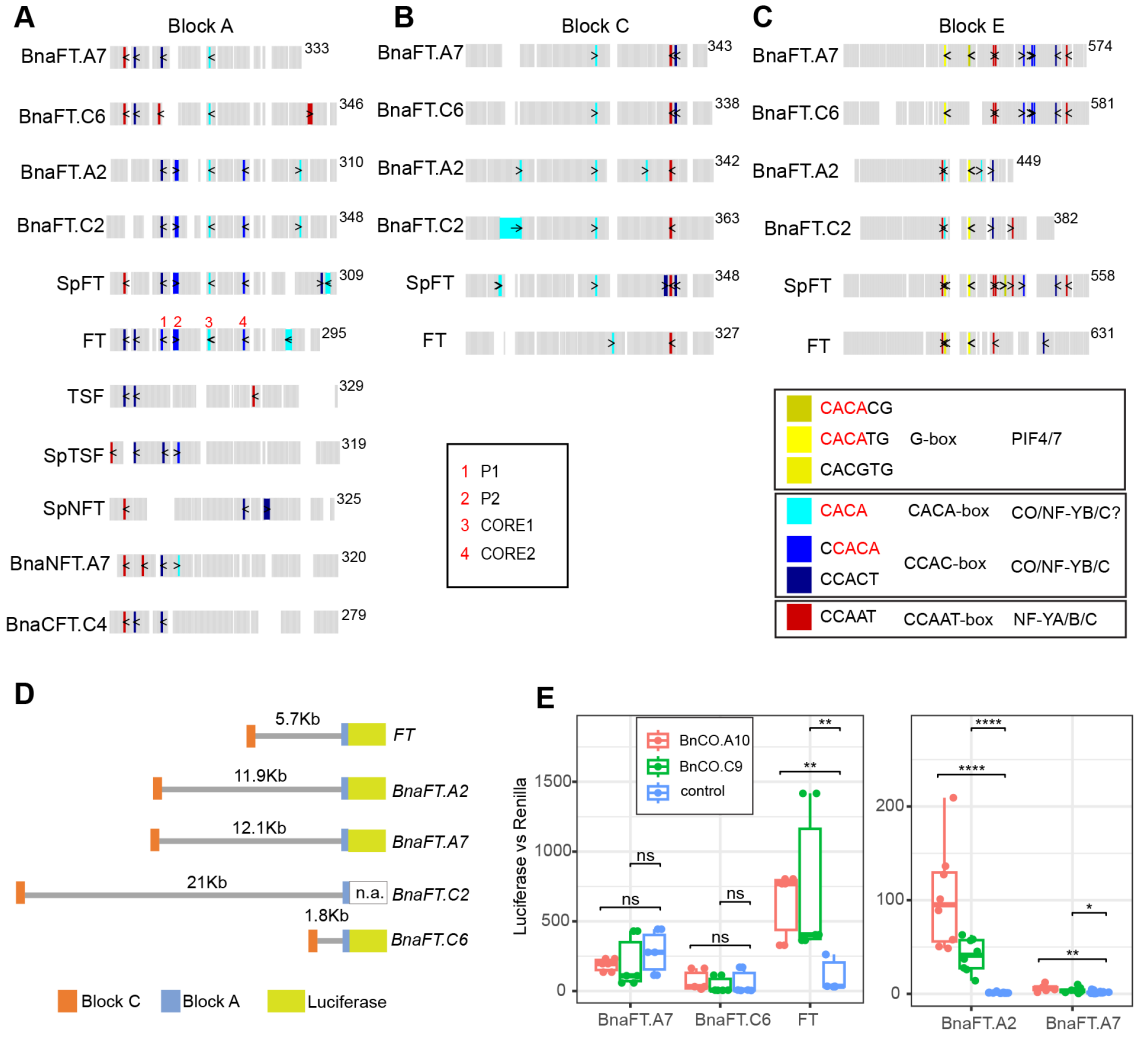


**Figure 4. Conservation of the cis-regulatory code at *B. napus FT* homologs.**
Schematic diagram showing the distribution of motifs within conserved blocks A **(A)**, C **(B)** and E **(C)** for *FT-like* genes from *A. thaliana, S. parvula* and *B. napus*. Gray boxes indicate aligned sequences, white spaces indicate alignment gaps. Cis-elements are marked in different colors as indicated in the common legend. The length of the unaligned sequences is shown after each alignment block. Red numbers above the position of motifs at *FT* block A indicate previously characterized functional motifs. **(D)** Scheme of the promoter region of *B. napus FT* genes fused to LUC. **(E)** Promoter-reporter transactivation assay in infiltrated tobacco leaves. Agrobacteria transformed with a binary vector containing promoter Firefly luciferase fusions and Renilla luciferase under the control of the CaMV 35S promoter were co-infiltrated with bacteria expressing either BnaCO.A10, BnaCO.C9 or an empty binary vector. Infiltrated areas were extracted and Luciferase vs Renilla luciferase activity quantified. Boxplots show relative firefly vs Renilla signal from 4 to 6 independent infiltrations, the median is indicated as line, data-points as dots. Statistical analysis was performed using the non-parametric Wilcocxon signed rank test with FDR correction.

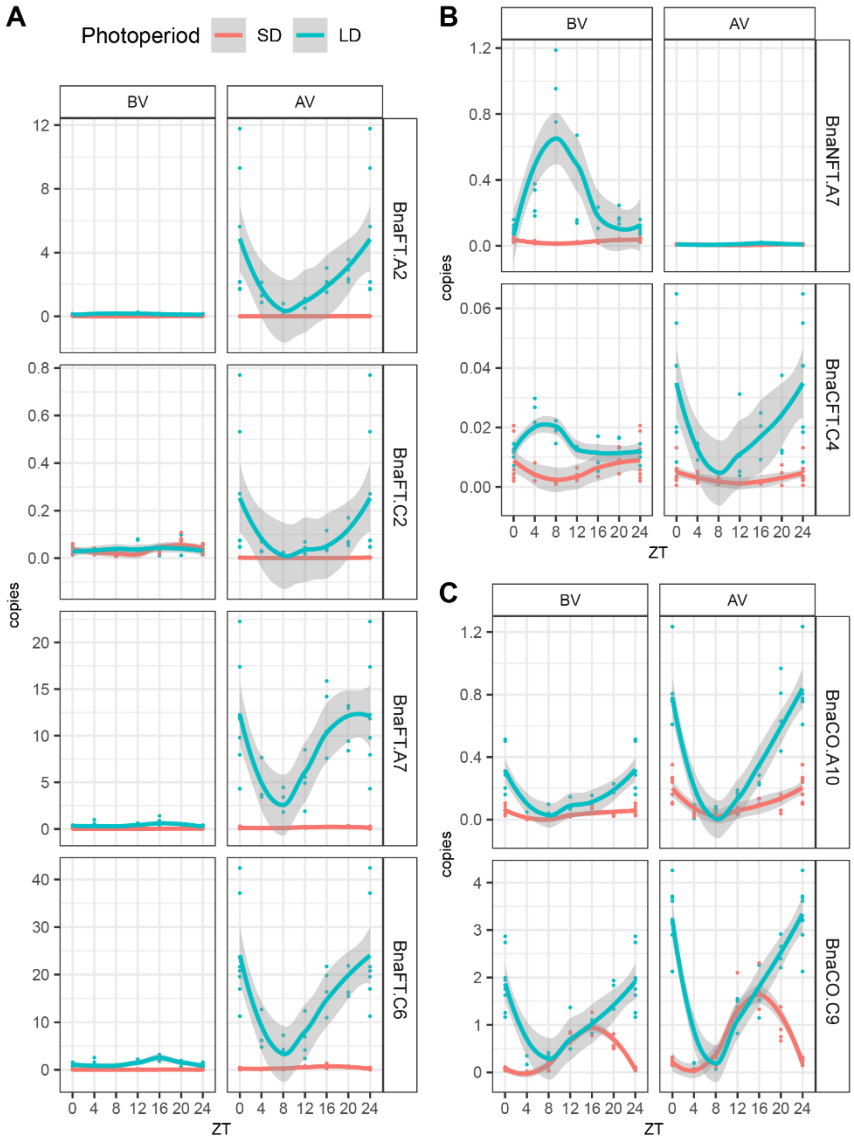


**Figure 5. Diurnal expression of *B. napus* *FT* and *CO* homologs in ZS11. (A)** Diurnal expression of *BnaFT.A2*, *BnaFT.C2*, *BnaFT.A7*, *BnaFT.C6*. **(B)** Diurnal expression of *BnaNFT.A7* and *BnaCFT.C4*. **(C)** Diurnal expression of *BnaCO.A10* and *BnaCO.C9*. Material from leaf 6 and leaf 8 were sampled every 4 h from ZS11 plants grown in SD and LD photoperiod in growth chambers at 22°C before (BV) and after (AV) vernalization, respectively. Time is plotted in reference to Zeitgeber (light on). Expression levels were analysed by gene-specific qRT-PCR using four independent biological replicates using genomic DNA as common reference point. *BnaENTH* was used to correct for differences in cDNA amount. Values for ZT0 and ZT24 were pooled at both time points. Data points are indicated as dots, lines were generated using a loess smoothing function, grey shapes indicate ± standard error.

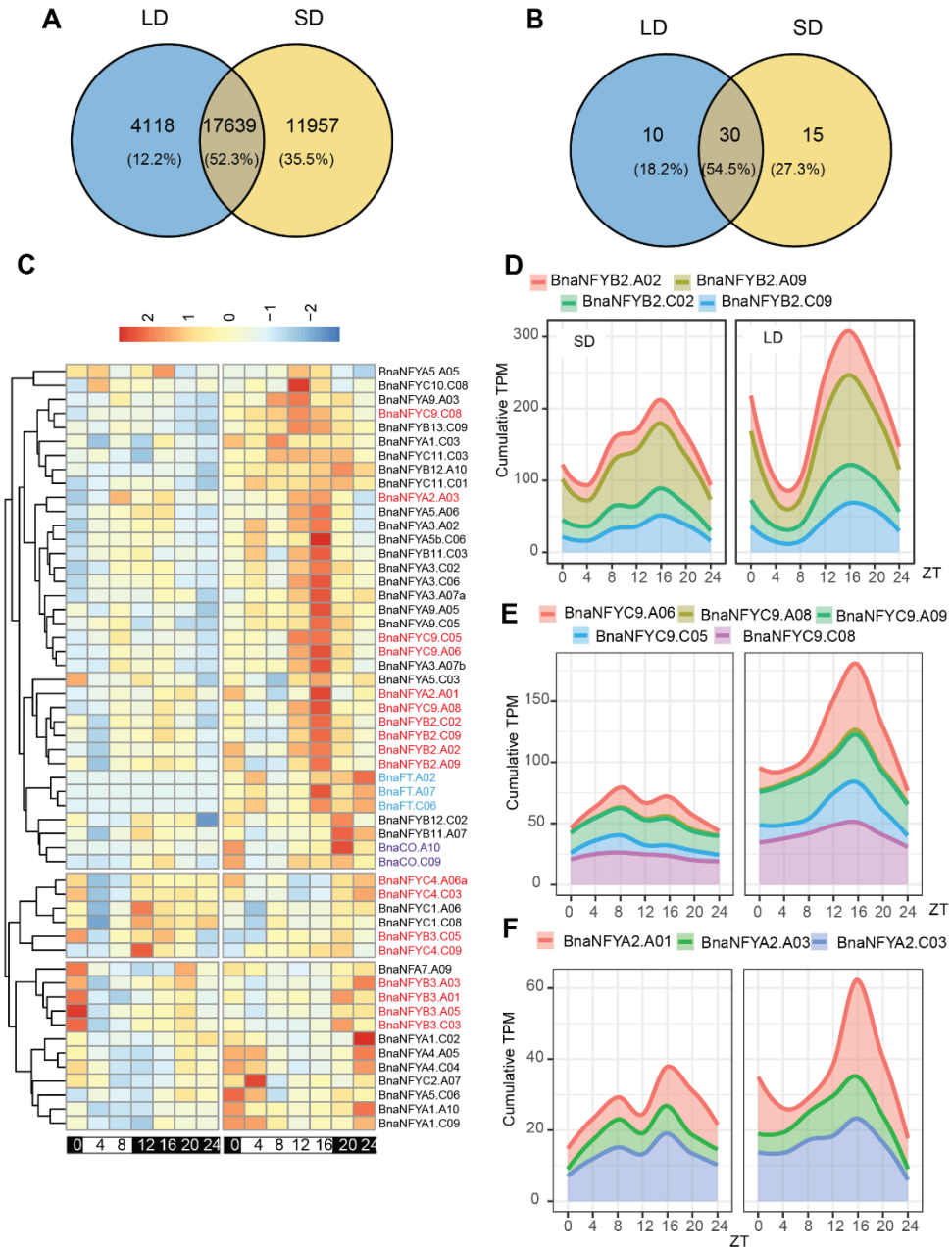


**Figure 6. Diurnal expression of *B. napus* NF-Y homologs. (A)** Venn diagram showing rhythmically expressed genes in LD and SD photoperiod. **(B)** As A) for NF-Y genes. **(C)** Heatmap of rhythmically expressed *B. napus* NF-Y genes after hierarchical clustering based on expression patterns. Expression data in TPM were normalized across all samples per gene, clustering was performed using the Manhattan distance metric. Colours indicate *B. napus* homologs of *NF-Y*s involved in *FT* regulation (red), *BnaFT*s (blue) and *BnaCO*s (purple). **(D)** Cumulative sum plot of TPM values in SD (left panel) and LD (right panel) for all *BnaNFYB2* genes. **(E)** as D) for *BnaNF-YC9* genes. **(F)** as D) for *BnaNF-YA2* genes.